

FINITE-SIZE EFFECTS ON THE  
CHARACTERIZATION OF FRACTAL SETS II:

$f(\alpha)$  construction via box counting on a two-scaled

snowflake fractal

**Jan Håkansson\***

*Nordisk Institut for Teoretisk Atomfysik,*

Blegdamsvej 17, DK-2100 Copenhagen Ø, Denmark

and

*Institute of Theoretical Physics,*

Chalmers University of Technology, S-412 96 Göteborg, Sweden

**Abstract** - We study box-counting on finite fractal sets and investigate the convergence of the multifractal  $f(\alpha)$  spectrum when varying the degree of resolution. As model of a two-dimensional multifractal aggregate, we use a simple two-scaled snowflake fractal for which the  $f(\alpha)$  spectrum may be found analytically---the exact result is compared with the box-counting solution on the finite levels.

## Introduction

Most previous characterizations of multifractals [1, 2] have brought a global description of the scaling properties through the determination of the continuous spectrum of scaling indices  $\alpha$  and their densities  $f(\alpha)$ . The  $f(\alpha)$  spectrum is related to the generalized fractal dimension  $D_q$ , the Renyi dimension [3], via a Legendre transformation [1].

A great deal of theoretical and experimental interest has developed in a variety of non-equilibrium growth processes and pattern formation (see e.g., [4] - [7] and references therein). Much attention has been paid to the study of the geometrical properties of highly ramified clusters formed in apparently unrelated physical, chemical and biological processes. Most of the numerical analysis of growing patterns have focused on the particular meaningful dimensions: the *Hausdorff* dimension  $D_0$ , the *information* dimension  $D_1$  and the *correlation* dimension  $D_2$ . Only very recently has more attention been paid to the computation of the whole spectrum of generalized dimensions [8], [9]. *Self-similar fractals* are fractals such that all the  $D_q$ 's coincide i.e., their  $f(\alpha)$  spectrum displays singularities of unique strength  $\alpha = D_q$ . In contrast, *multifractals* are usually characterized by a monotonic decreasing dependence of  $D_q$  versus  $q$ ; hence  $\alpha$  is no longer unique but may take on values in a finite range  $[\alpha_{min}, \alpha_{max}]$ , while  $f(\alpha)$  turns out to be, in general, a single humped function with  $D_0$  as its maximum. Measurements of the  $D_q$ 's and the  $f(\alpha)$  spectrum provide global statistical information about the scaling properties of fractals. The scaling exponent  $\alpha$  measures how fast the mass within a box decreases, as the box-size is reduced. It therefore measures the "strength of a singularity" for box-sizes  $l \rightarrow 0$ , i.e., in the thermodynamic limit of an infinite number of points within a finite volume. The  $f(\alpha)$  spectrum therefore identifies the underlying singularities and quantifies their relative contributions.

To calculate the generalized dimensions and the  $f(\alpha)$  spectrum, box-counting is perhaps the simplest and the most common method. In an earlier work [10], we have studied the  $f(\alpha)$  construction via box-counting on a two-scaled Cantor set, and showed how to obtain the optimal  $f(\alpha)$  spectrum by varying the box-sizes. In the present paper we apply the general ideas of [10] to the study of finite-size effects on a slightly more realistic model of a fractal aggregate; a simple two-scaled snowflake fractal. This two-dimensional extension of the Cantor set model used in [10] is a further example of a *finite* fractal consisting of a finite number of objects with finite sizes. We investigate the effects of finite particle size in box-counting by varying the degrees of resolution, and calculate the optimal  $f(\alpha)$  spectrum. We also use the box-counting solution to calculate the rate of convergence of the  $f(\alpha)$  approximation. With our specific choice of length-scales, it is possible to find analytic expressions for the generalized dimensions  $D_q$  and the  $f(\alpha)$  spectrum and we may solve the complete box-counting problem. It is then easy to compare successive approximations of the  $f(\alpha)$  spectrum with

the exact result, and thereby calculate the convergence rate of the  $f(\alpha)$  approximations.

### Box counting

To use box-counting, we cover the  $d$ -dimensional fractal object with a grid of boxes, all with the same size  $l^d$ , and calculate the probability to find a measure in each box. We use the so called *fixed radius (fixed volume) method* in contrast to the *fixed mass method* [11]. In general, the optimal dividing of the fractal object is found by minimizing the number of boxes with a non-zero measure. This is obvious, since the approximation of the Hausdorff dimension given by box-counting on any level  $n$  is defined as

$$D_0^{(n)} = -\frac{\ln N^{(n)}(l)}{\ln l} \quad (1)$$

where  $N^{(n)}(l)$  is the number of non-empty boxes of length  $l$ , and the fact that the box-counting approximation of  $D_0^{(n)}$  is always greater than the exact value of  $D_0$ . The reason for the inequality  $D_0^{(n)} > D_0$  is that all boxes, filled or unfilled, are taken with same weight, since  $q = 0$ . So by minimizing  $N^{(n)}(l)$ , we can find the best approximation of  $D_0$  (and  $D_q$  for  $q > 0$ ) on any level  $n$ .

If we let  $N$  be the total number of non-empty boxes,  $M$  the total number of particles (the total mass), and  $N_i$  the total number of measures (particles) in the  $i$ 'th box, the  $f(\alpha)$ -spectrum is given by [1,10]

$$f(\alpha(q)) = q\alpha(q) - \tau(q) \quad (2)$$

where

$$\tau(q) = \frac{1}{\ln l} \cdot \ln \sum_{i=1}^{N(l)} \left(\frac{N_i}{M}\right)^q \quad (3)$$

and

$$\alpha(q) = \frac{d\tau(q)}{dq} = \frac{1}{\ln l} \cdot \frac{\sum_{i=1}^{N(l)} \left(\frac{N_i}{M}\right)^q \ln \left(\frac{N_i}{M}\right)}{\sum_{i=1}^{N(l)} \left(\frac{N_i}{M}\right)^q} \quad (4)$$

As was pointed out in [10], it is in general impossible to identify single particles in an observed image. Instead one may define a smallest "particle" size, or resolution, being an estimate of the size of the smallest observable single "particle", and then create a new image built up of these "particles". This procedure gives a smallest relevant grid size for the box-counting. If the image is digitized, there is a natural finest resolution given by the digitization grid.

### Exact box-counting on the snowflake fractal

We will now study the box-counting problem for the finite snowflake fractal on an arbitrary level  $n$ . The snowflake fractal in Fig. 1 can be generated by the operator  $\hat{T}$  defined by

$$\hat{T}x = 4xl + xL \quad (5)$$

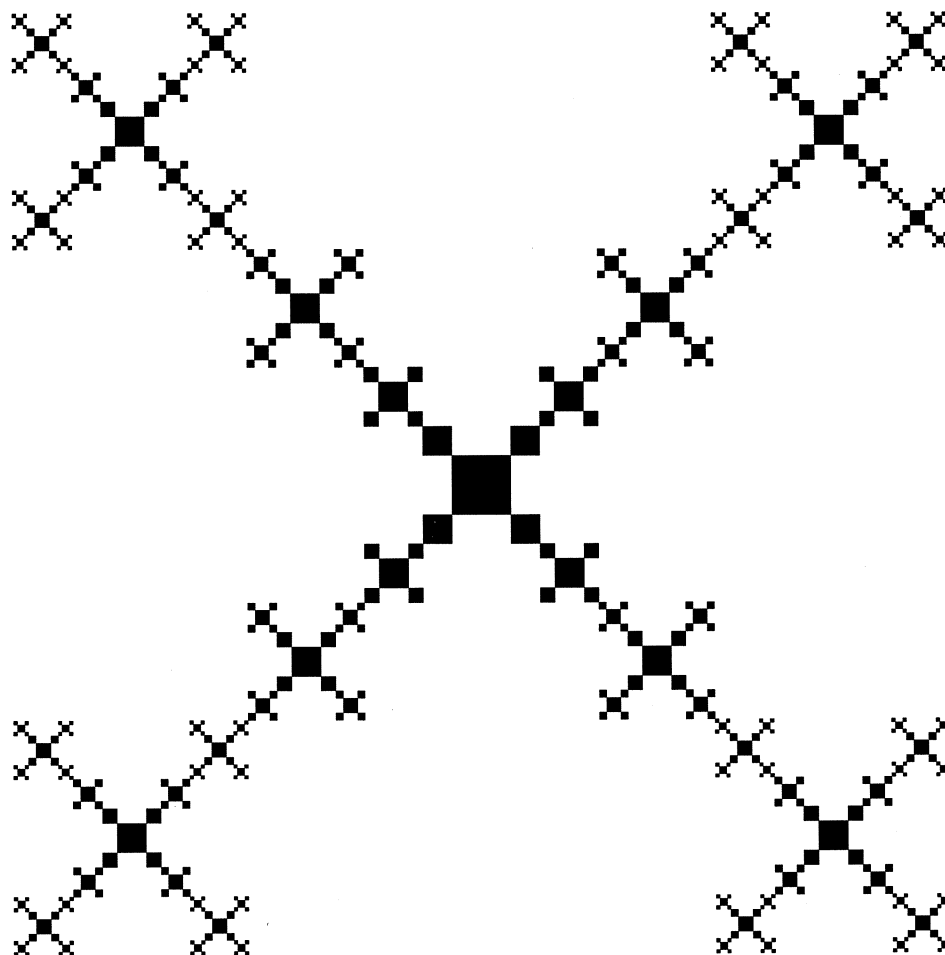


Figure 1. A two-dimensional snowflake fractal with two rescalings. The fractal is constructed by dividing a square of size one into 16 equal squares of size  $1/4$  and removing all squares except the four in the middle, which now form a large square, and the four in the corners. Successive divisions of each new squares into five new ones give this pattern. The fractal object is shown on level four, i.e., after four successive divisions.

If we let the operator act on a unit square, i.e.,  $x \equiv 1$  we get  $4l + L$ , which means four new squares of size  $l (= 1/4)$  and one of size  $L (= 1/2)$ . This is the first level of the set, and higher levels are found by further operation of  $\hat{T}$ . Level three for instance, is given by

$$\begin{aligned}
\hat{T}^3(l) &= \hat{T}^2(4l + L) \\
&= \hat{T}(16l^2 + 4lL + 4Ll + L^2) \\
&= 64l^3 + 16l^2L + 16lLl + 16Ll^2 + 4lL^2 + 4LlL + 4L^2l + L^3
\end{aligned}$$

On the finest resolution of level three, (see Fig. 2) we have 512 non-empty boxes of size  $l_B = l/64$ , with configuration

$$\begin{array}{cccc}
(64)\frac{1}{1}l^3 & (64)\frac{1}{4}l^2L & (64)\frac{1}{4}lLl & (64)\frac{1}{16}lL^2 \\
(64)\frac{1}{4}lL^2 & (64)\frac{1}{16}lLl & (64)\frac{1}{16}L^2l & (64)\frac{1}{64}L^3
\end{array}$$

m=6	$(64)\frac{1}{1}l^3$	$(64)\frac{1}{4}l^2L$	$(64)\frac{1}{4}lLl$	$(64)\frac{1}{16}lL^2$	$(64)\frac{1}{4}Ll^2$	$(64)\frac{1}{16}LlL$	$(64)\frac{1}{16}L^2l$	$(64)\frac{1}{64}L^3$
m=5	$(64)\frac{1}{1}l^3 + (16)\frac{1}{4}l^2L$		$(16)\frac{1}{1}lLl$	$(16)\frac{1}{4}lL^2$	$(16)\frac{1}{1}Ll^2$	$(16)\frac{1}{4}LlL$	$(16)\frac{1}{4}L^2l$	$(16)\frac{1}{16}L^3$
m=4	$(16)\frac{4}{1}l^3 + (1)\frac{1}{1}l^2L$		$(16)\frac{1}{1}lLl + (1)\frac{1}{4}lL^2$		$(16)\frac{1}{1}Ll^2 + (1)\frac{1}{4}LlL$		$(4)\frac{1}{1}L^2l$	$(4)\frac{1}{4}L^3$
m=3	$(4)\frac{4}{1}l^3 + (1)\frac{1}{1}l^2L + (1)\frac{1}{1}lLl + (1)\frac{1}{4}lL^2$				$(4)\frac{4}{1}Ll^2 + (1)\frac{1}{1}LlL$		$(4)\frac{1}{1}L^2l + (1)\frac{1}{4}L^3$	
m=2	$(4)\frac{16}{1}l^3 + (4)\frac{1}{1}l^2L + (4)\frac{1}{1}lLl + (1)\frac{1}{1}lL^2$				$(4)\frac{4}{1}Ll^2 + (1)\frac{1}{1}LlL + (1)\frac{1}{1}L^2l + (1)\frac{1}{4}L^3$			
m=1	$(4)\frac{16}{1}l^3 + (4)\frac{1}{1}l^2L + (4)\frac{1}{1}lLl + (1)\frac{1}{1}lL^2 + (4)\frac{1}{1}Ll^2 + (1)\frac{1}{1}LlL + (1)\frac{1}{1}L^2l + (1)\frac{1}{4}L^3$							
m=0	$64l^3 + 16l^2L + 16lLl + 4lL^2 + 16Ll^2 + 4LlL + 4L^2l + L^3$							

Table 1. This table shows the contents in the boxes for different box-sizes for the snow-flake fractal on level 3. We can also see how to add particles from one level to another. The length of the boxes is given by  $(1/2)^m$ . The number in the brackets denotes the number of a certain box-configuration.

The probability measure in the non-empty boxes are the same on this level, since the box-size is the same as the size of the "particles". We define a "particle" as the smallest square at the finest resolution, i.e., the squares of size  $l^n$ , where  $n$  denote the level of the set. This means that only one "particle" fits into a box at this level ( $m = 6$  in Table 1). In Table 1, we show the contents in the boxes for different grid sizes of level  $n = 3$ . The number in the brackets is the number of a certain box configuration, i.e.,  $(16)[lLl + 1/4lL^2]$  means that we have 16 boxes with one  $lLl$ -particle and a  $1/4$  of an  $lL^2$ -particle.

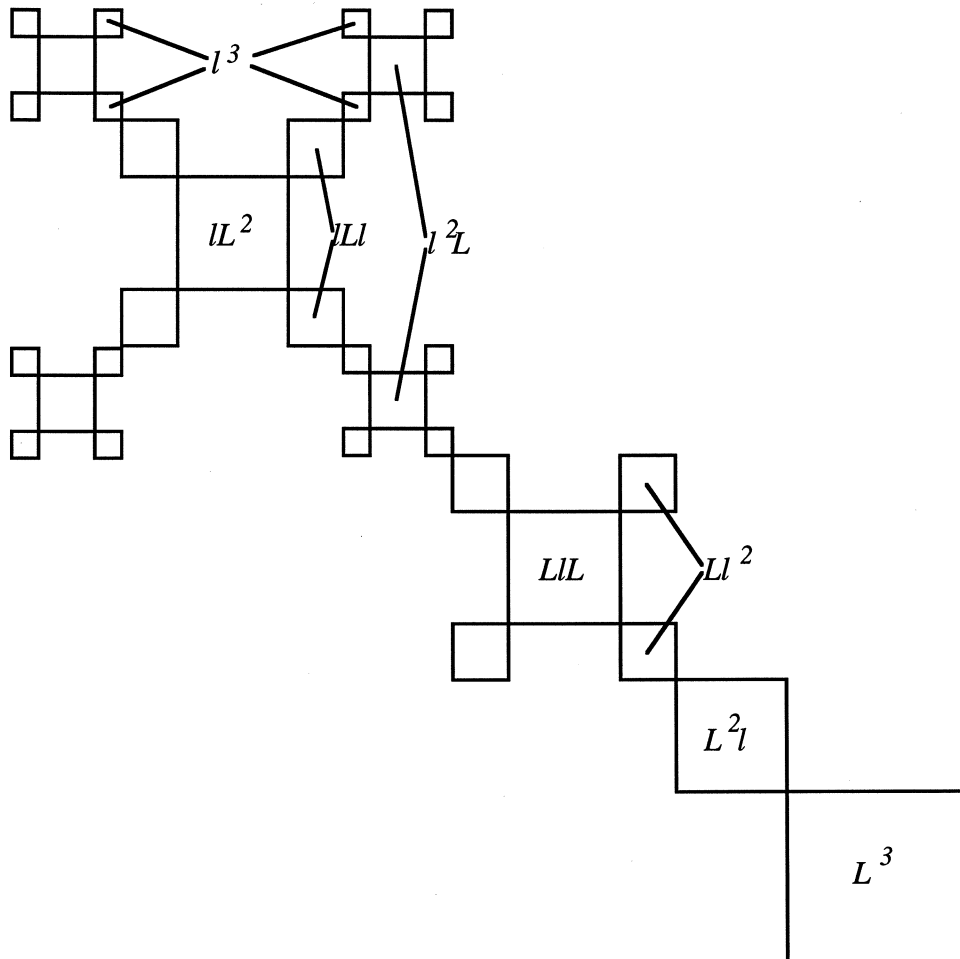


Figure 2. The snowflake fractal at level 3. Note that we show only a quarter of the entire fractal.

Since we know the total measure of the fractal on level  $n$  (which is  $(1/2)^n$ ), we can easily calculate the probability measure as the mass in a box divided by the total mass of the fractal, to get the partition sum on each level of resolution. For instance, the probability of a box containing  $lLl + (1/4)lL^2$  is given by

$$\frac{\left\{ \left(\frac{1}{4}\right)^2 \left(\frac{1}{2}\right)^2 \left(\frac{1}{4}\right)^2 + \frac{1}{4} \left(\frac{1}{4}\right)^2 \left(\left(\frac{1}{2}\right)^2\right)^2 \right\}}{\left(\frac{1}{2}\right)^3} = \frac{1}{64}$$

For a general level  $n$  of the fractal set (i.e., after  $n$  operations of  $\hat{T}$  on a unit square) the complete box-counting problem can be solved, for any box-size  $(1/2)^m$ , for  $m=1,2, \dots, 2n$  in the following five steps;

- 1) Use the operator  $\hat{T}^n$  to find the configuration of the snowflake fractal at level  $n$ , where  $l^n$  becomes the smallest "particle" with the size  $(1/4)^n$ .

2) Partition all the "particles" of sizes greater than  $(1/4)^n$ , to pieces of size  $(1/4)^n$ , as shown for box-level  $m = 6$  in *Table 1*.

3) For each level  $m$  add the "particles" as illustrated in *Table 1* to find the configuration at all levels  $m=1,2, \dots, 2n$  (i.e., for all box-sizes  $l = 1/2, 1/4, \dots, (1/2)^{2n}$ ). We know for instance that the  $l^2L$ -box must be a neighbour to the  $l^3$ -box (see *Fig. 2*).

4) Calculate the probability measure in the boxes on each level, to construct the partition sum  $\Gamma$ , and

5) use the Eqs. (2) - (4) to calculate the spectrum of scaling indices  $f(\alpha)$ .

It is now a straightforward analysis to find recursive relations for the coefficients and the probability measures for a general level  $n$ . If we let  $m$  be the box-level, we get the following partition sum

$$\Gamma_n^{(m)} = 2^{m\tau} \sum_{i=1}^N a_i^{(m)} \{p_i^{(m)}\}^q \quad (6)$$

where  $N$  is given by

$$N = \begin{cases} m & m \leq n \\ n+1 & m > n \end{cases} \quad (7)$$

From Eq. (3) we then get

$$\tau(q)_n^{(m)} = -\frac{1}{m \ln 2} \ln \left\{ \sum_{i=1}^N a_i^{(m)} \{p_i^{(m)}\}^q \right\} \quad (8)$$

and from Eq. (4)

$$\alpha_n^{(m)} = -\frac{1}{m \ln 2} \cdot \frac{\sum_{i=1}^N a_i^{(m)} \{p_i^{(m)}\}^q \cdot \ln \{p_i^{(m)}\}}{\sum_{i=1}^N a_i^{(m)} \{p_i^{(m)}\}^q} \quad (9)$$

and finally we get the  $f(\alpha)$  spectrum

$$f_n^{(m)}(\alpha_n^{(m)}) = q\alpha_n^{(m)} - \tau_n^{(m)}(q) \quad (10)$$

The generalized dimensions are given by

$$(D_n^{(m)})_q = \frac{\tau_n^{(m)}(q)}{q-1} \quad (11)$$

and, in particular the Hausdorff dimension



$$(D_n^{(m)})_0 = \frac{1}{m \ln 2} \ln \left\{ \sum_{i=1}^N a_i^{(m)} \right\} \quad (12)$$

See appendix for the calculations of the coefficients  $a_i^{(j)}$ .

In the calculation of the  $f(\alpha)$  spectrum, we find two different families, due to the symmetry of the snowflake fractal. The reason is that boxes of length  $(1/4)^m$  matches the smallest particles (i.e., those in the corners) to give the correct  $\alpha$ -value. In Fig. 3 and Fig. 4, we show the exact  $f(\alpha)$  curve [10]

$$\alpha(q) = 2 + \frac{8 \cdot 2^{-q}}{\sqrt{1+16 \cdot 2^{-q}} - 1 - 16 \cdot 2^{-q}} \quad (13)$$

$$f(\alpha(q)) = \frac{8q \cdot 2^{-q}}{\sqrt{1+16 \cdot 2^{-q}} - 1 - 16 \cdot 2^{-q}} - \frac{1}{\ln 2} \ln \left\{ \frac{\sqrt{1+16 \cdot 2^{-q}} - 1}{8} \right\} \quad (14)$$

compared with successive approximations  $f_n^{(m)}(a_n^{(m)})$  for the two families on level  $n = 16$ . The odd family consists of the boxes of size  $(1/2)^m$  where  $m$  is an odd number, and the even family corresponds to those for which  $m$  is an even number. On this level, the snowflake fractal consists of  $8^{16}$  "particles" of size  $4^{-16}$ .

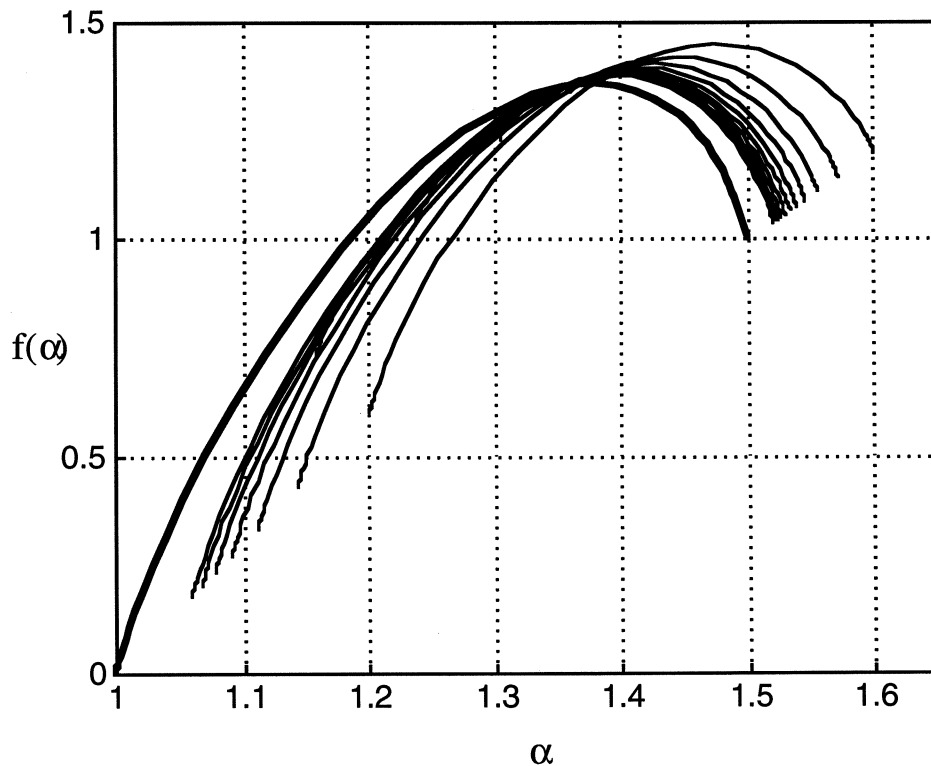


Figure 3. The exact  $f(\alpha)$  spectrum (thick line) compared with the solutions from the box-counting for the even family on resolution-level 16 (thin lines).

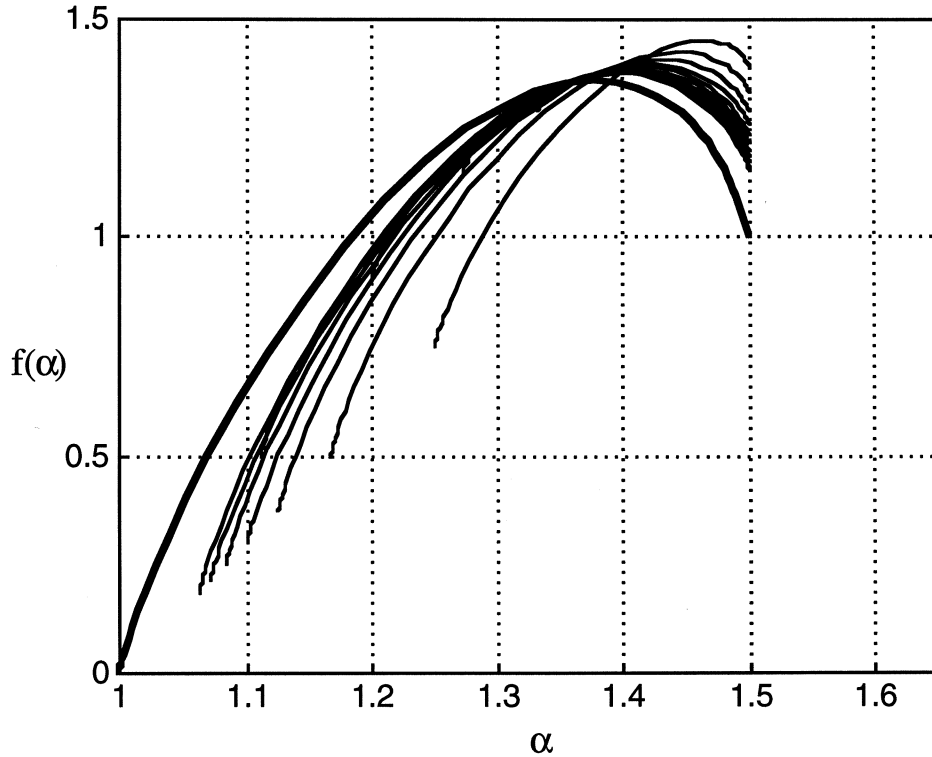


Figure 4. The exact  $f(\alpha)$  spectrum (thick line) compared with the solutions from the box-counting for the odd family on resolution-level 16 (thin lines).

We also observe that for negative  $q$ -values the best approximation of the  $f(\alpha)$  spectrum is given by the result from small boxes, and for  $q > 0$  the best result is given by boxes of the same size as the largest particle in the set (i.e., the  $L^n$ -particle). It is therefore easy to find the optimal approximation of an  $f(\alpha)$  spectrum by varying the size of the boxes.

### The convergence of the $f(\alpha)$ spectrum

To calculate the convergence of the  $f(\alpha)$  spectrum from the box-counting solution, we will consider the two limits  $q \rightarrow -\infty$  and  $q \rightarrow +\infty$  where simple analytic expressions may be found. From Eqs. (13) and (14) we have the exact values

$$(\alpha, f) \Big|_{q \rightarrow -\infty} = (1, 3/2) \quad (15)$$

and

$$(\alpha, f) \Big|_{q \rightarrow +\infty} = (0, 0) \quad (16)$$

and we want to calculate the distance between these points and the points, given by the box-counting with different resolutions. From the box-counting calculation we have

$$(\alpha, f)_{q \rightarrow -\infty}^{(m)} = \frac{1}{m \ln 2} (-\ln p_{\min}^{(m)}, \ln \alpha_{\min}^{(m)}) \quad (17)$$

and

$$(\alpha, f)_{q \rightarrow +\infty}^{(m)} = \frac{1}{m \ln 2} (-\ln p_{\max}^{(m)}, \ln \alpha_{\max}^{(m)}) \quad (18)$$

respectively, where

$$p_{\min}^{(m)} = \left(\frac{1}{2}\right)^{[(3m+1)/2]} \quad (19)$$

$$\alpha_{\min}^{(m)} = \begin{cases} 2^{m+1} & m \text{ odd} \\ \left(\frac{m+2}{2}\right) 2^m & m \text{ even} \end{cases} \quad (20)$$

and

$$p_{\max}^{(m)} = \left(\frac{1}{2}\right)^{m+1} \quad (21)$$

$$\alpha_{\max}^{(m)} = 2^3 \quad m \leq n + 1 \quad (22)$$

For  $m > n+1$ ,  $\alpha_{\max}^{(m)}$  is not trivially given, but can be found from the recursive relations in the appendix.

In Eq. (20) we can distinguish between the two families, (the odd and the even) shown in Fig. 3 and Fig. 4 and we have

$$(\alpha, f)_{q \rightarrow -\infty}^{(m)} = \begin{cases} \left(\frac{3}{2} + \frac{1}{2m}, 1 + \frac{1}{m}\right) & m \text{ odd} \\ \left(\frac{3}{2}, 1 + \frac{\ln(1+m/2)}{m \ln 2}\right) & m \text{ even} \end{cases} \quad (23)$$

and

$$(\alpha, f)_{q \rightarrow +\infty}^{(m)} = \left(1 + \frac{1}{m}, \frac{3}{m}\right) \quad m \leq n + 1 \quad (24)$$

The distance to the exact values are then given by

$$d^{(m)}(q \rightarrow -\infty) = \begin{cases} \frac{\sqrt{5}}{2m} & m \text{ odd} \\ \frac{\ln(1+m/2)}{m \ln 2} & m \text{ even} \end{cases} \quad (25)$$

and

$$d^{(m)}(q \rightarrow +\infty) = \frac{\sqrt{10}}{m} \quad m \leq n+1 \quad (26)$$

We then get the convergence

$$d(l) \propto \frac{1}{\ln(1/l)} \quad (27)$$

for the odd family  $d^{(m)}(q \rightarrow -\infty)$  and for  $d^{(m)}(q \rightarrow +\infty)$ , ( $m < n+1$ ) where  $l$  is the size of the boxes. For the even family the convergence is slower (for box-sizes  $> 1/8$ ) due to the factor  $[(m+2)/2]$  in Eq. (20).

In Fig. 5 we show a plot of  $\ln(1/d(l))$  versus  $\ln(\ln(1/l))$  for both the families when  $q \rightarrow -\infty$ , where the odd family gives the straight line with slope 1. The convergence for  $q \rightarrow +\infty$ , is shown in Fig. 6, where the straight line represents the values  $m < n+1$ . Remark how well both families overlap. From the box-counting solution in the previous section it is possible to calculate the convergence for any values of  $q$ , and in Fig. 7 we show the convergence of the Hausdorff dimension,  $D_0$  to the exact value [10]

$$D_0^{\text{exact}} = \frac{\ln\left(\frac{\sqrt{17}-1}{8}\right)}{\ln 2}$$

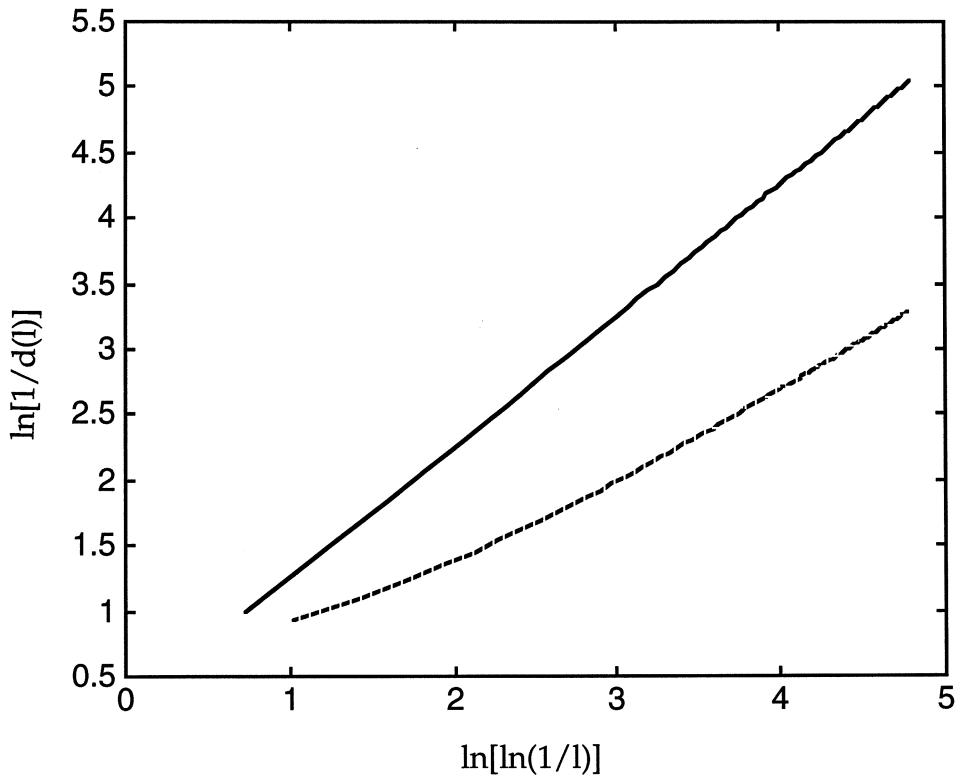


Figure 5. The convergence of  $f(\alpha)$  for  $q \rightarrow -\infty$  is illustrated in this plot of  $\ln(1/d(l))$  vs  $\ln(\ln(1/l))$ . The odd family is the solid curve, and the even family the dashed curve.

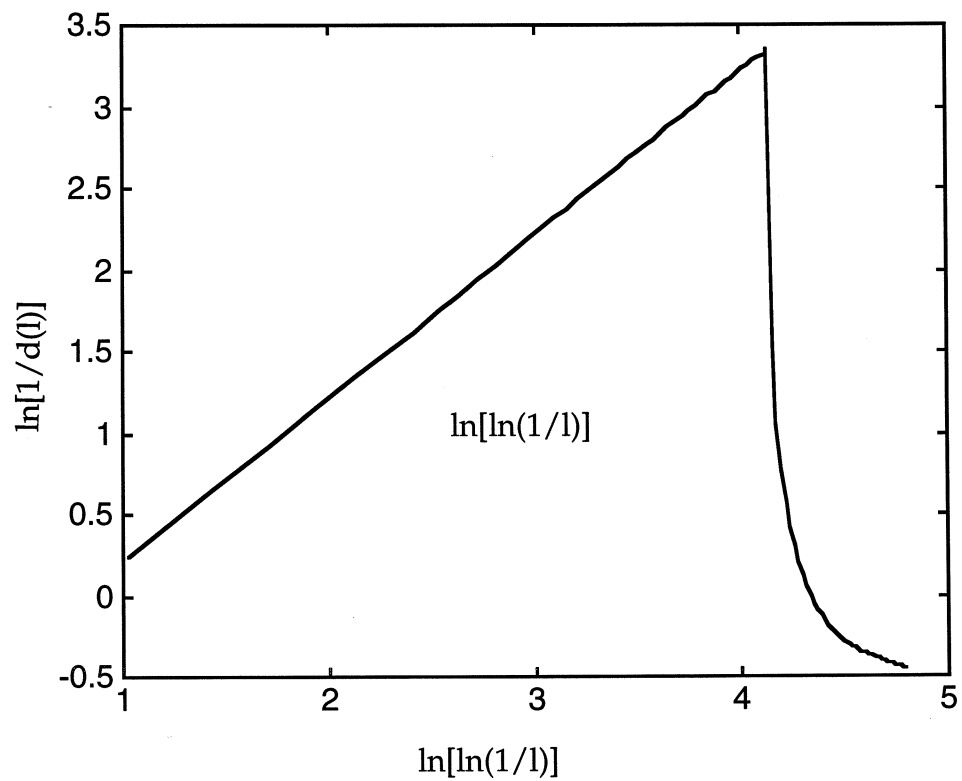


Figure 6. The convergence of  $f(\alpha)$  for  $q \rightarrow +\infty$  is the same as for  $q \rightarrow -\infty$  except for  $m > n+1$  (the left part of the figure). The two families overlap and have the same convergence.

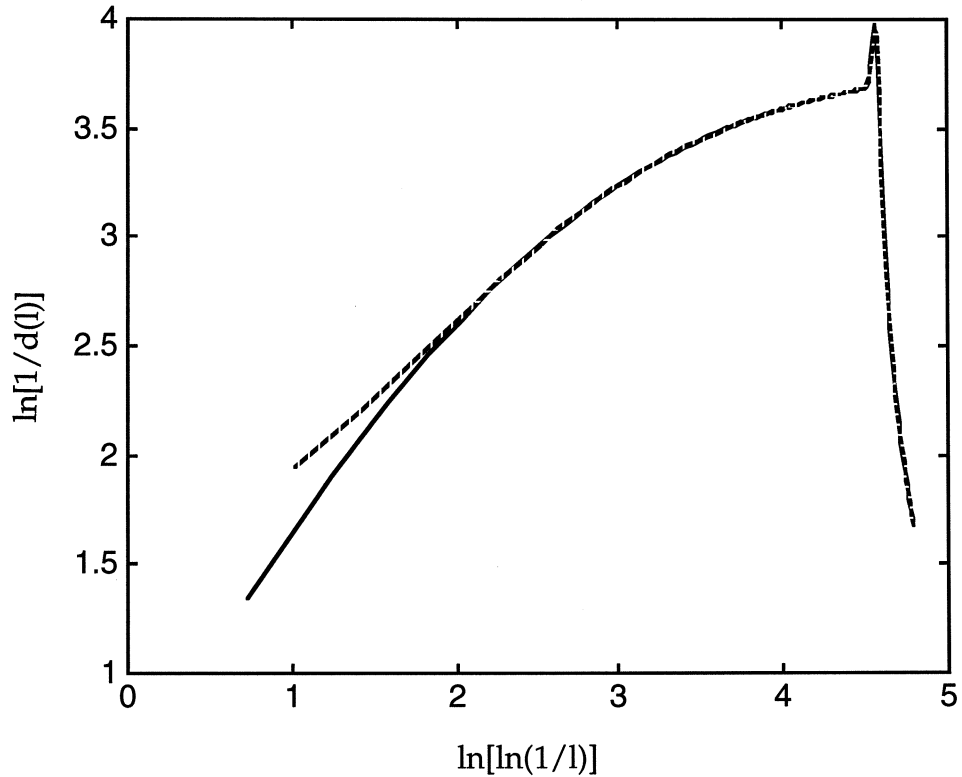


Figure 7. The convergence of the Hausdorff dimension  $D_0$  is shown for the two families. The dashed curve represents the even family.

### Concluding remarks

Real fractal objects, like aggregates, show fractal properties only within a certain interval of length scales. This is due to the finite number of particles and finite-size effects. The structure becomes non-fractal for length scales comparable to the lattice length, as well as outside some typical correlation length. When partitioning a two-dimensional image (e.g., a projection, like a transmission electron micrograph of aggregated Co particles [12]), the effect of the finite particle size will play an important role for the determination of the  $f(\alpha)$  spectrum, especially for negative  $q$ -values. This is due to the finite resolution and the fact that the boxes will not be necessarily centered on particles (objects) of the fractal. Some of the boxes will contain a vanishingly small measure, giving unreasonably large contribution to the partition sum for large negative  $q$ -values. We have used a two-dimensional, two-scaled fractal set at finite levels to model a fractal aggregate. The simple choice of length scales in our model makes it possible to solve the complete box-counting problem on any level of resolution. From the box-counting solution and the exact given  $f(\alpha)$  spectrum, we can calculate the convergence of the box-counting approximation. Due to the symmetry of our model, we find two different families of  $f(\alpha)$  spectrum. The convergence properties for the two families are very much the same, especially for box-sizes smaller than the largest particle (i.e., the square in the middle, see Fig. 1) of the set. To find the optimal approximation, one

should use only boxes smaller than the largest particles in the set, which gives the best approximation for  $q > 0$ . Larger boxes do not resolve the details of the fractal structure. For negative  $q$ -values, one must vary the box-size to find the optimal approximation, and for a given value of  $f$  one should select the smallest  $\alpha$ -value. The slow convergence (see Eq. (27)) shows that a very large number of points (particles) is needed to get an accurate  $f(\alpha)$  spectrum from an experiment. However, an experimental fractal image, (e.g., a micrograph of aggregated particles) is not fractal on length-scales larger than some correlation length and there is often a maximum number of particles of the order  $10^3$ . For negative  $q$ -values the convergence will then not be as good as for the snowflake on which we are able to place our boxes in an optimal way.

### Acknowledgments

This work was partially supported by grants from the Swedish Natural Science Research Council. I am very grateful to G. Russberg, M. H. Jensen and P. Cvitanovic' for stimulating discussions, and G Niklasson for the valuable experimental assistance.

### Appendix

To find recursive relations for the coefficients ( $a_i^{(j)}$ ) in the box-counting solution, we first reexpressed them as

$$a_i^{(j)} = c_i^{(j)} \cdot 4^{b_i^{(j)}} \quad (28)$$

It is then easy to find separate recursive relation for  $c_i^{(j)}$  and  $b_i^{(j)}$ . We find the following recursive relation for the coefficients  $c_i^{(j)}$

$$c_i^{(j)} = c_i^{(j-2)} + c_{i-1}^{(j-1)} \quad (29)$$

for the indices

$$\begin{cases} j = 3, \dots, n; & i = 2, \dots, j \\ j = n+1, \dots, 2n; & i = 2, \dots, 2(n+1) - j \end{cases} \quad (30)$$

and the following recursive relation

$$c_i^{(j)} = c_i^{(j-1)} \quad (31)$$

for the indices

$$j = n+2, \dots, 2n; \quad i = 2n+3-j, \dots, n+1$$

The initial values of the coefficients  $c_i^{(j)}$  in the recursive relations above is given by

$$\begin{cases} c_1^{(j)} = 1; \\ c_2^{(2)} = 1 \end{cases} \quad j = 1, 2, \dots, 2n \quad (32)$$

Finally, the second coefficients  $b_i^{(j)}$  in Eq. (28) is given by

$$b_i^{(j)} = \left[ \frac{j+2-i}{2} \right] \quad (33)$$

for the indices

$$\begin{cases} j = 1, \dots, n; \\ j = n+1, \dots, 2n; \end{cases} \quad \begin{cases} i = 1, \dots, j \\ i = 1, \dots, 2(n+1) - j \end{cases} \quad (34)$$

and by the recursive relation

$$b_i^{(j)} = b_i^{(j-1)} + 1 \quad (35)$$

for the indices

$$j = n+2, \dots, 2n; \quad i = 2n+3-j, \dots, n+1$$

where the brackets [ ] denote the integer part. For the probability measures in the boxes, which are given by the mass in a certain box divided by the total mass of the fractal, we find the recursive relation

$$p_i^{(j)} = \frac{1}{2} p_{i-1}^{(j-1)} \quad (36)$$

for the indices

$$\begin{cases} j = 2, \dots, n+1; \\ j = n+2, \dots, 2n; \end{cases} \quad \begin{cases} i = 2, \dots, j \\ i = 2, \dots, 2(n+1) - j \end{cases} \quad (37)$$

and the recursive relation

$$p_i^{(j)} = \frac{1}{4} p_i^{(j-1)} \quad (38)$$

for the indices

$$j = n+2, \dots, 2n; \quad i = 2n+3-j, \dots, n+1$$

The initial values for the probabilities is given by

$$p_i^{(j)} = \left( \frac{1}{2} \right)^{[(3j+1)/2]} \quad j = 1, 2, \dots, 2n \quad (39)$$

where the brackets [ ] denotes the integer part.



$$\begin{cases} c_1^{(j)} = 1; \\ c_2^{(2)} = 1 \end{cases} \quad j = 1, 2, \dots, 2n \quad (32)$$

Finally, the second coefficients  $b_i^{(j)}$  in Eq. (28) is given by

$$b_i^{(j)} = \left[ \frac{j+2-i}{2} \right] \quad (33)$$

for the indices

$$\begin{cases} j = 1, \dots, n; \\ j = n+1, \dots, 2n; \end{cases} \quad \begin{cases} i = 1, \dots, j \\ i = 1, \dots, 2(n+1) - j \end{cases} \quad (34)$$

and by the recursive relation

$$b_i^{(j)} = b_i^{(j-1)} + 1 \quad (35)$$

for the indices

$$j = n+2, \dots, 2n; \quad i = 2n+3-j, \dots, n+1$$

where the brackets [ ] denote the integer part. For the probability measures in the boxes, which are given by the mass in a certain box divided by the total mass of the fractal, we find the recursive relation

$$p_i^{(j)} = \frac{1}{2} p_{i-1}^{(j-1)} \quad (36)$$

for the indices

$$\begin{cases} j = 2, \dots, n+1; \\ j = n+2, \dots, 2n; \end{cases} \quad \begin{cases} i = 2, \dots, j \\ i = 2, \dots, 2(n+1) - j \end{cases} \quad (37)$$

and the recursive relation

$$p_i^{(j)} = \frac{1}{4} p_i^{(j-1)} \quad (38)$$

for the indices

$$j = n+2, \dots, 2n; \quad i = 2n+3-j, \dots, n+1$$

The initial values for the probabilities is given by

$$p_i^{(j)} = \left( \frac{1}{2} \right)^{[(3j+1)/2]} \quad j = 1, 2, \dots, 2n \quad (39)$$

where the brackets [ ] denotes the integer part.

## References

- [1] T. C. Halsey, M. H. Jensen, L. P. Kadanoff, I. Procaccia and B. I. Shraiman, *Phys. Rev. A* **33**, 1141 (1986)
- [2] P. Collet, J. L. Lebowitz, and A. Porzio, *J. Stat. Phys.* **47**, 609 (1987)
- [3] A. Renyi, *Probability Theory*, North Holland, Amsterdam (1970)
- [4] H. E. Stanley and N. Ostrowski, eds., *On growth and form: fractal and nonfractal patterns in physics*, Reidel, Dordrecht, (1986)
- [5] L. Pietroniero and E. Tosatti, eds., *Fractal in physics*, North-Holland, Amsterdam, (1986)
- [6] H. E. Stanley, ed., *Statphys 16*, North-Holland, Amsterdam, (1986)
- [7] W. Göttinger and G. Dangelmayr, eds., *The physics of structure formation*, Springer, Berlin, (1987)
- [8] P. Meakin and S. Havlin, *Phys. Rev. A* **36**, 4428 (1987)
- [9] F. A. Arnedo, G. Grasseau and H. L. Swinney, *Self-similarity of diffusion-limited aggregation and electrodeposition cluster*, preprint (1988)
- [10] J. Håkansson and G. Russberg, *Phys. Rev. A* **41**, 1855 (1990)
- [11] P. Grassberger, R. Badii and A. Politi, *J. Stat. Phys.* **51**, 135 (1988)
- [12] G. A. Niklasson, A. Torebring, C. G. Granqvist and T. Farestam, *Phys. Rev. Lett.* **60**, 1735 (1988)